Food Chemistry 457 (2024) 140098

Contents lists available at ScienceDirect

Food Chemistry

journal homepage: www.elsevier.com/locate/foodchem

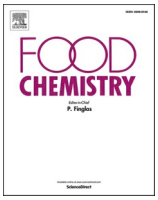

Comparison of sea buckthorn fruit oil nanoemulsions stabilized by protein-polysaccharide conjugates prepared using β-glucan from various sources

Ziyi Shen [a,1], Juan Dai [b,1], Xinyue Yang [a], Yao Liu [a], Lei Liu [a], YuKun Huang [a], Lijun Wang [a], Pengfei Chen [a], Xianggui Chen [a], Chisong Zhang [d], Juan Zhao [e], Xiao Yang [a,*], Qin Wang [c,*]

[a] School of Food and Bioengineering, Xihua University, Chengdu, 610039, PR China
[b] School of Laboratory Medicine, Chengdu Medical College, Chengdu, 610500, PR China
[c] Department of Nutrition and Food Science, University of Maryland, College Park, MD 20742, United States
[d] Chengdu Academy of Agriculture and Forestry Sciences, Chengdu, 610500, PR China
[e] Sichuan Synlight Biotech Ltd., Chengdu, 610000, PR China

ARTICLE INFO

Keywords:
Glycosylation conjugates
O/W nanoemulsion
Stability
In vitro digestion

ABSTRACT

To understand the influence of β-glucans structure on the emulsifying properties of protein-polysaccharide conjugates, sodium caseinate (NaCas) was utilized to form glycosylation conjugates with varying degrees of glycosylation (10.68–17.50%) using three β-glucans from bacteria, yeast, and oats. This process induced alterations in the secondary structure of protein. The nanoemulsions prepared with the glycosylated conjugates exhibited superior stability compared to those formulated solely with NaCas, particularly under conditions of drastic pH fluctuations and extended storage periods. The nanoemulsion prepared with the NaCas-Salecan conjugate demonstrated exceptional stability at pH 4 and 6, or storage for 20 days. Additionally, it significantly attenuated the oxidation of unsaturated fatty acids and exhibited the lowest levels of aggregation, flocculation, and free fatty acid release rate during *in vitro* digestion. This study suggested the potential of the NaCas-Salecan conjugates in enhancing the stability of nanoemulsions and facilitating the colorectal-targeted delivery of sea buckthorn fruit oil.

1. Introduction

Sea buckthorn fruit oil is a functional oil extracted from *Hippophae rhamnoides* L. pulp, rich in bioactive substances such as unsaturated fatty acids, carotenoids, phytosterols and tocopherols (Chang et al., 2020). Research indicates its anti-inflammatory, antioxidative, immune-enhancing and cardiovascular and cerebrovascular-protective properties (Dong, Binosha Fernando, Durham, Stockmann, & Jayasena, 2023; Olas, 2018; Vilas-Franquesa, Saldo, & Juan, 2020; Wang, Xu, & Liao, 2022). However, the oil's instability and susceptibility to oxidation shorten its shelf life, produce off-flavors, and constrain its applications and market value (Waglewska, Misiaszek, & Bazylinska, 2022).

Oil-in-water nanoemulsions can enhance the stability and bioavailability of lipophilic functional nutrients by inhibiting lipid oxidation and providing more binding sites for digestive enzymes (such as lipase) (Islam et al., 2023; Rave, Echeverri, & Salamanca, 2020; Tereshchuk, Starovoitova, Vyushinsky, & Zagorodnikov, 2022). Emulsion stability, crucial for retaining functional components, is largely determined by the choice of emulsifier. (Xu, Mukherjee, & Chang, 2018). Protein-polysaccharide conjugates formed *via* the Maillard reaction offer promising potential as emulsifiers and stabilizers in food systems, exhibiting improved solubility, emulsifying properties, thermal stability, foaming ability, and gel properties (Nooshkam, Varidi, Zareie, & Alkobeisi, 2023).

Previous studies utilized β-glucans from various sources to enhance protein functionality *via* the Maillard reaction (de Oliveira, Coimbra, de Oliveira, Zuniga, & Rojas, 2016; Sun et al., 2019). β-Glucans differ in glycosidic bonds and molecular weights based on their sources. For instance, the β-glucan from cereals consist of β (1 → 3) and β (1 → 4) linkages, while yeast β-glucan contain β (1 → 3) and β (1 → 6) linked

* Corresponding authors.
E-mail addresses: yangxiao@mail.xhu.edu.cn (X. Yang), wangqin@umd.edu (Q. Wang).
[1] Zhiyi Shen and Juan Dai contributed equally to this work

https://doi.org/10.1016/j.foodchem.2024.140098
Received 14 March 2024; Received in revised form 22 May 2024; Accepted 12 June 2024
Available online 15 June 2024

branches. Bacterial β-glucans exhibit diverse chemical structures, ranging from linear to branched forms. Linear bacterial β-glucans consist of repetitive glucose units linked *via* β (1 → 3) bonds, while branched bacterial β-glucan contain glucose units connected by β (1 → 3,1 → 6) linkages (Kaur, Sharma, Ji, Xu, & Agyei, 2020). The structural disparities among β-glucans may influence the properties of protein-polysaccharide conjugates in emulsion preparation. However, comparative studies between β-glucans with different structures or sources are rarely reported.

In this study, three different sources of β-glucan (from bacteria, yeast, and oat) were utilized to form protein-polysaccharide conjugates with sodium caseinate, and sea buckthorn fruit oil nanoemulsions were prepared using these glycosylated conjugates. The above gap is addressed by elucidating the impact of different β-glucan sources on emulsion stability and functionality. This study provides insights into the development and utilization of sea buckthorn fruit oil and β-glucan glycosylated emulsifiers, and also provides a theoretical basis for optimizing the formulation of sea buckthorn fruit oil functional foods and improving their efficacy.

2. Materials and methods

2.1. Materials

Sea buckthorn fruit oil was purchased from Xinjiang Altay Food Co., Ltd. (Altay, China). Salecan (CAS 1439905–58-4, average MW 2.0 MDa), a natural β-glucan from bacteria consisting of seven residues linked by β-(1 → 3)/α-(1 → 3) glycosidic bonds, was obtained from Sichuan Hetai Xinguang Biotechnology Co., Ltd. (Chengdu, China). Beta-glucan from yeast (CAS 9012-72-0, MW 27.9–175 kDa) and β-glucan from oats (CAS 9041-22-9, average MW 1.6 MDa) were purchased from Henan Bangsu Biotechnology Co., Ltd. (Zhengzhou, China). Sodium caseinate (NaCas, CAS 9005-46-3, from milk), sodium taurocholate (CAS 145–42-6), pepsin (CAS 9001-75-6, EC 3.4.23.1), bile extracts (CAS 8008-63-7), and lipase (CAS 9001–62-1, EC 3.1.1.3) were purchased from Sigma Aldrich (Shanghai, China). Phosphate-buffered saline (PBS), Nile red and SDS-PAGE gels were purchased from Shanghai Sangon Biotech Co., Ltd. (Shanghai, China). Methanol (chromatographic purity) was purchased from Thermo Fisher Scientific, Inc. (Waltham, MA, USA). Simulated gastric fluid (SGF) and simulated intestinal fluid (SIF) were purchased from Phygene Lifesciences Technology Co., Ltd. (Fuzhou, China).

2.2. Preparation of protein-polysaccharide conjugates

Protein-polysaccharide conjugates were prepared following previous reports (Capar & Yalcin, 2021). Briefly, NaCas and β-glucan (mass ratio of 1:1) were dissolved in ultrapure water to form a 1% (*w/v*) protein-polysaccharide mixture. The mixture was thoroughly dissolved by stirring for 2 h and hydrated at 4 °C overnight. Then the pH of the mixture was adjusted to 8, and the mixture was stirred at 90 °C for 90 min. The reaction was terminated by rapid cooling to room temperature, followed by freeze-drying to obtain glycosylated conjugates.

The degree of glycosylation (DG) was determined based on the alteration in the quantity of free amino groups before and after the reaction (Ding, Yan, Yu, & Liu, 2023). Specifically, 0.1 mL of sample solution was mixed with 2.7 mL of o-phthalic aldehyde (OPA) reagent and incubated for 1 min at room temperature. The absorbance was subsequently measured at 340 nm. The DG was calculated according to Eq. (1):

$$DG\ (\%) = (A_0 - A_t/A_0 \times 100\% \quad (1)$$

where A_0 is the absorbance value before glycosylation and A_t is the absorbance value after glycosylation.

2.3. Preparation of sea buckthorn fruit oil nanoemulsions

The preparation of sea buckthorn fruit oil nanoemulsions refers to previous reports (Rave et al., 2020). The NaCas-β-glucan conjugates were prepared in a 1% (*w/v*) aqueous solution, stirred for 2 h to ensure complete dissolution, and hydrated overnight at 4 °C. Then, the aqueous solution was mixed with sea buckthorn fruit oil at a volume ratio of 9:1 and sheared at 13,000 rpm/min for 5 min using an ULTRA-TURRAX T25 homogenizer (IKA, Staufen, Germany). The mixture was homogenized in a NanoGenizer 30 K high-pressure microfluidizer (Genizer, USA) twice at 15,000 psi and 6 °C to prepare the sea buckthorn fruit oil nanoemulsion. An emulsion prepared with unglycosylated NaCas was used as a control.

2.4. SDS–page

SDS–PAGE analysis was performed on the protein-polysaccharide conjugates using a 5% concentrated gel and 12% separating gel, and stained with Coomassie Brilliant Blue R-250, refers to previous reports (Zhang, Gong, Khanal, Lu, & Lucey, 2017).

2.5. Fluorescence spectroscopy

Fluorescence spectroscopy was obtained refers to previous reports (Sofronova, Semenyuk, & Muronetz, 2019). Two milligrams of protein-polysaccharide conjugates were dissolved in 1 mL of phosphate buffer solution (20 mmol/mL, pH 7.0), and the fluorescence emission spectra were measured using a FluoroMax-4 spectrofluorometer (Horiba Scientific, Japan) at room temperature. The excitation wavelength was 295 nm, and the emission spectra were collected in the range of 310–450 nm, with both excitation and emission wavelength slits of 5.0 nm.

2.6. Circular dichroism (CD) spectroscopy

CD spectroscopy was obtained refers to previous reports (Ding et al., 2023). Two hundred micrograms of protein-polysaccharide conjugates were dissolved in 1 mL of phosphate buffer solution (20 mmol/mL, pH 7.0). The secondary structure of the protein was analyzed using a Chirascan Plus circular dichroism spectrometer (Applied Photophysics, UK) with a collection wavelength range of 190–250 nm and a resolution of 1.0 nm at 25 °C. Each sample was scanned three times. Distilled water was used as a blank control. The spectra were smoothed using the instrument software. The proportion of each secondary structure was calculated using CDNN software.

2.7. FTIR analysis

The FTIR spectra of the samples were analyzed using a Spectrum Two FTIR spectrophotometer (PerkinElmer, USA) with an attenuated total reflectance (ATR) probe at a pressure of 70 Pa at room temperature. The wavelength range was 4000–650 cm^{-1}, and the resolution was 4 cm^{-1}.

2.8. Nanoemulsion particle size, PDI and ζ-potential

The average particle size, PDI value and ζ potential of the nanoemulsions were measured using a Zetasizer Nano ZS (Malvern, UK) at 25 °C after 100-fold dilution in ultrapure water. Emulsions with particle sizes beyond the measurement range of the Zetasizer were measured using a BetterSize 2600 laser particle size analyzer (Dandong Baxter, China) at a detector angle of 90°.

2.9. Fatty acid analysis by GC/MS

Fatty acid analysis refers to previous reports (Zheng et al., 2021). Five hundred microliters of sample were mixed with 2 mL of n-hexane for sonication extraction and then centrifuged at 5000 rpm for 10 min.

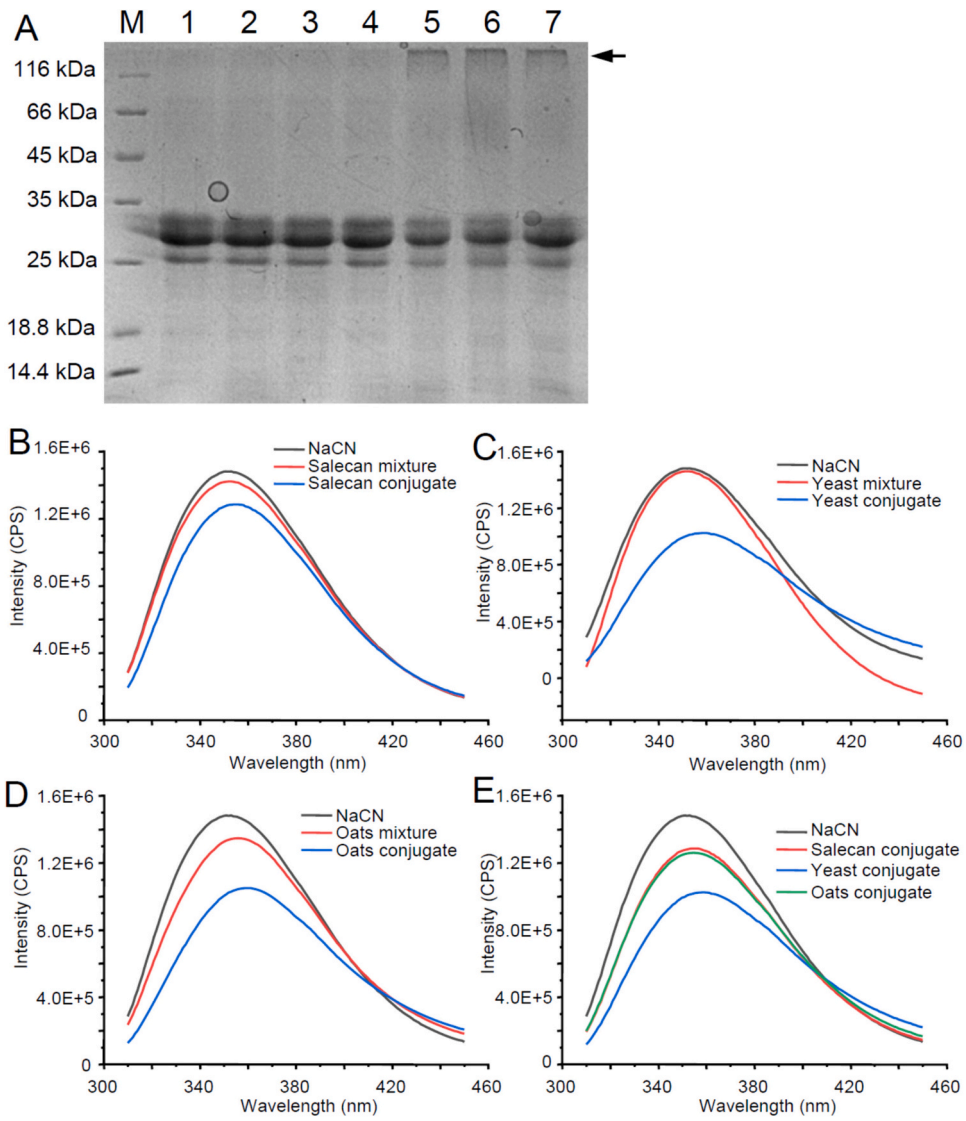

Fig. 1. (A) SDS–PAGE analysis of NaCas, three mixtures and three conjugates. Lanes M ~ 7 are the standard protein marker, NaCas, Salecan mixture, yeast mixture, oats mixture, Salecan conjugate, yeast conjugate, and oats conjugate, respectively. (B-E) Intrinsic fluorescence emission spectra of NaCas, three mixtures and three conjugates. (NaCas: NaCas solution; Salecan mixture: the mixture of Salecan and NaCas; yeast mixture: mixture of yeast β-glucan and NaCas; oats mixture: mixture of oat β-glucan and NaCas; Salecan conjugate: NaCas-Salecan conjugates; yeast conjugate: NaCas-yeast β-glucan conjugates; oat conjugate: NaCas-oat β-glucan conjugates).

One milliliter of the upper organic phase was combined with 500 μL of 0.5 mol/L potassium hydroxide-methanol solution, and incubated at 80 °C for 10 min for methyl esterification. The product was centrifuged at 5000 rpm for 5 min, and the upper organic phase was filtered for GC/MS analysis.

The fatty acid composition was detected by a GCMS-QP2020 NX gas chromatograph-mass spectrometer (Shimadzu, Japan) equipped with an Rtx-5MS capillary column (30 mm × 0.25 mm i.d. × 0.25 μm, Restek, USA). Helium was used as the carrier gas at 0.8 mL/min. The injector temperature was 270 °C, and the split ratio was 20:1. The oven temperature was was held at 100 °C for 2 min, increased to 180 °C at a rate of 10 °C/min, was held at this point for 2 min, increased to 210 °C at a rate of 2 °C/min, and was held for 2 min. The MS interface temperature was 230 °C, and the ion source temperature was 200 °C. MS spectra were obtained in the range of *m/z* 35–500.

2.10. *In vitro* digestion model

The digestion characteristics of the sea buckthorn fruit oil nanoemulsions were assessed using a two-stage *in vitro* digestion model according to previous studies (Minekus et al., 2014).

In the gastric digestion stage, the sample was mixed with simulated gastric fluid (SGF, containing 6.9 mmol/L KCl, 0.9 mmol/L K_2HPO_4, 25 mmol/L $NaHCO_3$, 47 mmol/L NaCl, 0.1 mmol/L $MgCl_2$, 0.5 mmol/L $(NH_4)_2CO_3$, and 0.15 mmol/L $CaCl_2$) at a volume ratio of 1:1. Porcine pepsin (EC 3.4.23.1) was added to achieve a concentration of 2000 U/mL, and the solution was adjusted to pH 2.5. The mixture was incubated for 2 h at 37 °C with continuous shaking at 100 rpm.

In the intestinal digestion stage, the chyme from the mixture of the gastric digestion stage was combined with simulated intestinal fluid (SIF, containing 6.8 mmol/L KCl, 0.8 mmol/L K_2HPO_4, 85 mmol/L $NaHCO_3$, 38 mmol/L NaCl, 0.3 mmol/L $MgCl_2$, and 0.6 mmol/L $CaCl_2$) at a ratio of 1:1 (*V*/V). Bile extracts were added to achieve a concentration of 10 mmol/L, the pH of the solution was adjusted to 7.0. Porcine pancreatic lipase (EC 3.1.1.3) was added to attain a concentration of 2000 U/mL. The mixture was incubated for 2 h at 37 °C with continuous shaking at 100 rpm.

To assess the digestion of seabuckthorn fruit oil in the nano-

Table 1
The protein secondary structure of protein.

Sample	α-Helix(%)	Beta-Fold(%)	Beta-Turn (%)	Rndm.Coil (%)
NaCas	6.9 ± 0.17^{a}	41.7 ± 0.24^{a}	20.4 ± 0.24^{d}	32.5 ± 0.22^{c}
Salecan mixture	6.8 ± 0.27^{b}	41.4 ± 0.30^{ab}	20.4 ± 0.19^{d}	32.7 ± 0.23^{c}
Yeast mixture	7.2 ± 0.17^{a}	40.8 ± 0.22^{c}	20.9 ± 0.23^{c}	32.6 ± 0.20^{c}
Oats mixture	7.1 ± 0.18^{a}	41.3 ± 0.19^{b}	20.6 ± 0.26^{cd}	32.5 ± 0.19^{c}
Salecan conjugate	6.9 ± 0.22^{a}	38.8 ± 0.32^{d}	21.4 ± 0.23^{b}	33.6 ± 0.22^{b}
Yeast conjugate	7.1 ± 0.18^{a}	38.2 ± 0.24^{e}	21.7 ± 0.31^{ab}	33.8 ± 0.22^{ab}
Oats conjugate	7.1 ± 0.24^{a}	37.6 ± 0.28^{f}	21.9 ± 0.25^{a}	34.0 ± 0.19^{a}

Data presented are expressed as the mean ± SEM (n = 3). The different letters in each column represent a significant difference at $P < 0.05$. NaCas: NaCas solution; Salecan mixture: the mixture of Salecan and NaCas; Yeast mixture: the mixture of yeast β-glucan and NaCas; Oats mixture: the mixture of oat β-glucan and NaCas; Salecan conjugate: NaCas-Salecan conjugates; Yeast conjugate: NaCas-yeast β-glucan conjugates; Oats conjugate: NaCas-oat β-glucan conjugates.

emulsions, the liberation of free fatty acids (FFAs) resulting from lipid digestion was monitored employing a pH-stat method, as described in prior research (Borreani et al., 2017). The pH of the aforementioned mixture was maintained at 7.0 by titrating with NaOH using a T7 automatic titrator (Mettler-Toledo, Schwerzenbach, Switzerland). The consumption of NaOH was recorded to calculate the release of FFAs after the addition of lipase to the mixture using the following Eq. (2):

$$\text{FFAs}\ (\%) = \left(V_{NaOH(t)} \times C_{NaOH} \times MW_{oil}\right) / (2 \times M_{oil}) \times 100\% \quad (2)$$

where $V_{NaOH\ (t)}$ is the volume of NaOH consumed (L) at t min, C_{NaOH} is the concentration of NaOH (0.5 mol/L), MW_{oil} is the average molecular weight of sea buckthorn fruit oil (878.7 g/mol), and M_{oil} is the initial mass of sea buckthorn fruit oil (g) in the emulsions.

2.11. Data analysis

Each group of experiments was performed 3 times in parallel, and the data are expressed as the mean ± S.E.M. One-way analysis of variance (ANOVA) followed by Duncan's shortest significant range test was performed using SPSS 22.0 software (SPSS, Chicago, USA).

Table 2
Particle size, ζ-potential, PDI of the nanoemulsions.

Group	Size (nm)	PDI	Zeta (mV)
NaCas	255.27 ± 4.27^{b}	0.242 ± 0.010^{a}	−60.53 ± 1.40^{c}
Salecan mixture	269.73 ± 2.19^{a}	0.207 ± 0.010^{b}	−57.77 ± 0.93^{b}
Yeast mixture	255.37 ± 2.56^{b}	0.230 ± 0.011^{ab}	−61.47 ± 1.02^{c}
Oats mixture	251.87 ± 3.32^{b}	0.223 ± 0.014^{b}	−49.37 ± 0.99^{a}
Salecan conjugate	237.73 ± 3.04^{d}	0.178 ± 0.016^{c}	−60.00 ± 1.20^{c}
Yeast conjugate	242.97 ± 3.33^{c}	0.227 ± 0.011^{ab}	−65.33 ± 0.76^{d}
Oats conjugate	239.63 ± 3.65^{c}	0.189 ± 0.008^{c}	−64.33 ± 1.95^{d}

Data presented are expressed as the mean ± SEM (n = 3). The different letters in each column represent a significant difference at $P < 0.05$. NaCas: NaCas solution; Salecan mixture: the mixture of Salecan and NaCas; Yeast mixture: the mixture of yeast β-glucan and NaCas; Oats mixture: the mixture of oat β-glucan and NaCas; Salecan conjugate: NaCas-Salecan conjugates; Yeast conjugate: NaCas-yeast β-glucan conjugates; Oats conjugate: NaCas-oat β-glucan conjugates.

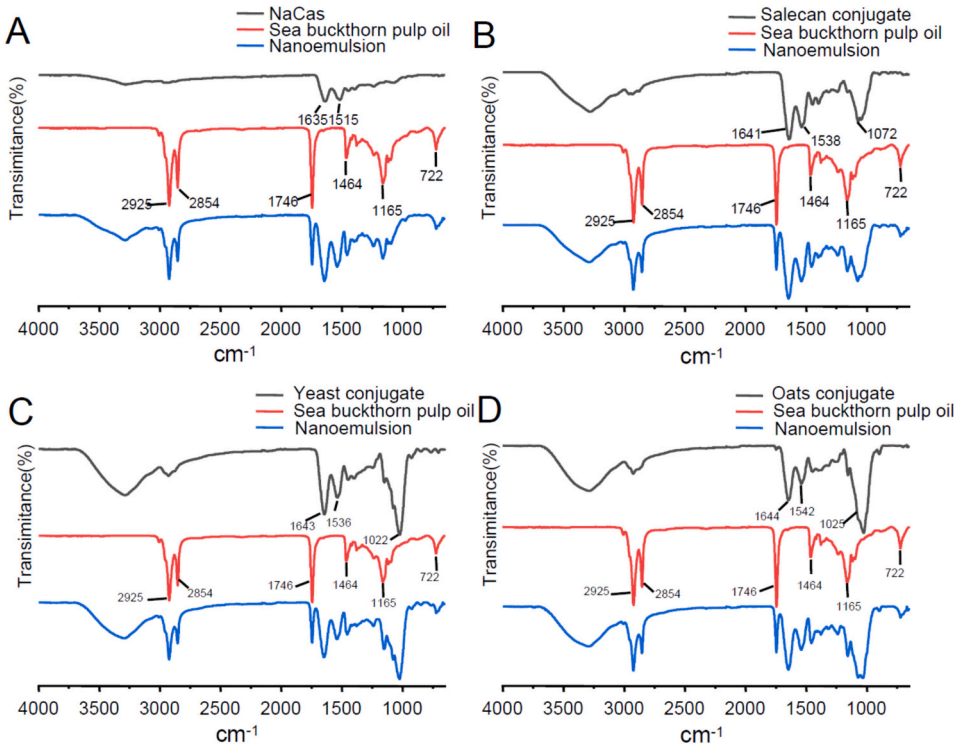

Fig. 2. Infrared spectra of sea buckthorn fruit oil nanoemulsions prepared with NaCas or three protein-polysaccharide conjugates. (A) Nanoemulsion prepared with NaCas. (B) Nanoemulsion prepared with NaCas-Salecan conjugates. (C) Nanoemulsion prepared with NaCas-yeast β-glucan conjugates. (D) Nanoemulsion prepared with NaCas-oat β-glucan conjugates. (NaCas: NaCas solution; Salecan conjugate: NaCas-Salecan conjugates; yeast conjugate: NaCas-yeast β-glucan conjugates; oat conjugate: NaCas-oat β-glucan conjugates).

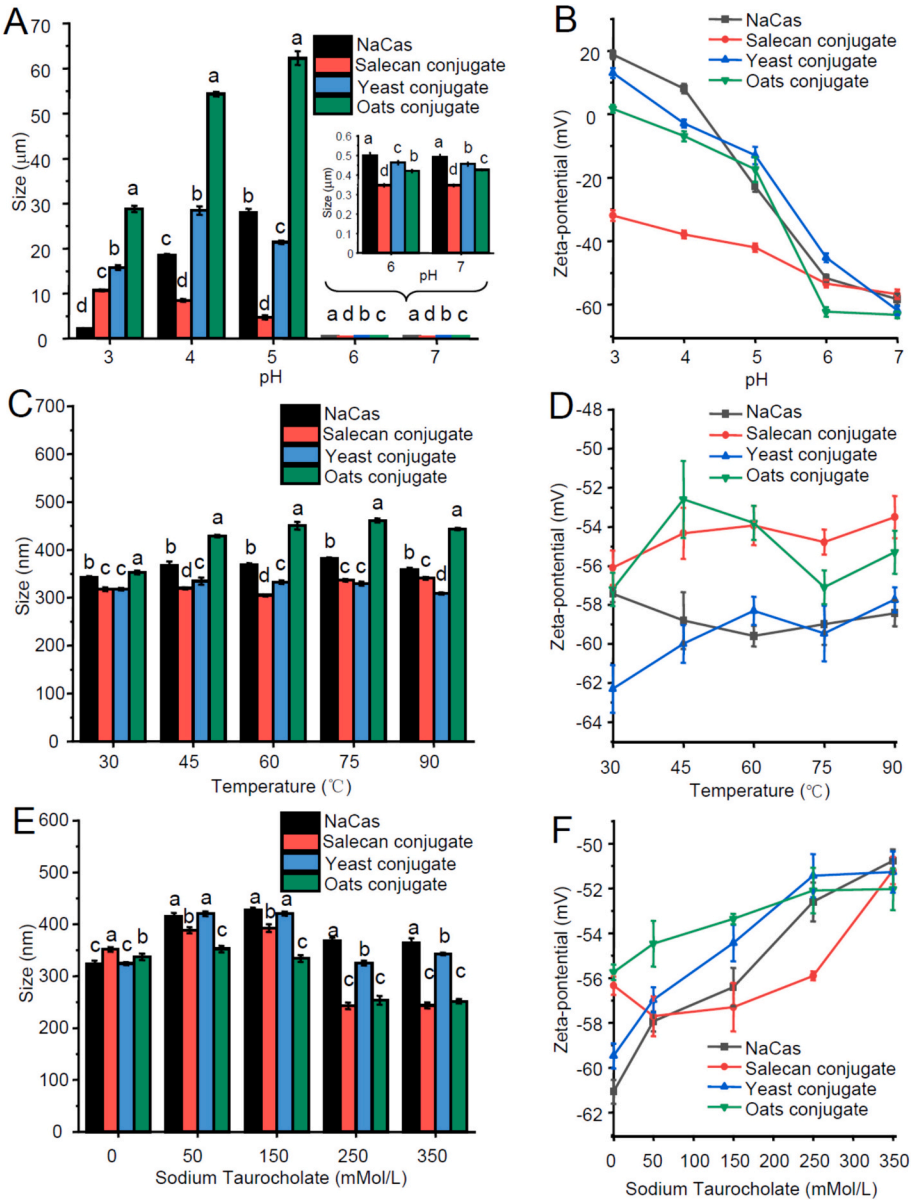

Fig. 3. Changes in the particle size (A, C, E) and ζ-potential (B, D, F) of sea buckthorn fruit oil nanoemulsions prepared with NaCas or three protein-polysaccharide conjugates at different pH values, temperatures and bile salt concentrations. Data presented are expressed as the mean ± SEM ($n = 3$). The different letters in same treatment represent a significant difference at $P < 0.05$. (NaCas: Nanoemulsion prepared with NaCas; Salecan conjugate: Nanoemulsion prepared with NaCas-Salecan conjugates; yeast conjugate: Nanoemulsion prepared with NaCas-yeast β-glucan conjugates; oat conjugate: Nanoemulsion prepared with NaCas-oat β-glucan conjugates).

3. Results and discussion

3.1. Characteristics of NaCas-β-glucan conjugates

As shown in Fig. 1A, the comparison between NaCas and the three mixtures of β-glucans with NaCas revealed no significant difference in the gel bands. However, the main bands in the lanes corresponding to the three NaCas-β-glucan conjugates appeared lighter, with evident bands observed at the top of the separation gel. Some studies have shown that the coupling of maltodextrin with glycosylated NaCas generates macromolecular polymers, which encounter difficulty in entering separation gels (Zhang et al., 2017). These results indicated that NaCas with the glycosylation of all three β-glucans resulted in the formation of macromolecular conjugates (NaCas with Salecan, yeast β-glucan, and oat β-glucan) were 14.98 ± 1.5%, 17.5 ± 3.54%, and 10.68 ± 0.94%, respectively.

The endogenous fluorescence emission spectra (Fig. 1B-E) revealed a significant reduction in fluorescence intensity for the three NaCas-β-glucan conjugates compared to NaCas and their respective mixtures. Given that tryptophan serves as fluorescent probe in proteins, NaCas features a solitary tryptophan residue (Trp157) situated within the protein's hydrophobic region (Mirdha & Chakraborty, 2019).This reduction in fluorescence intensity is attributed to the shielding effect exerted by covalent reaction of the polysaccharide with tryptophan, resulting in diminished absorption of tryptophan residues (Sofronova et al., 2019). Consequently, it suggests a covalent coupling reaction between NaCas and the three β-glucans, with the NaCas-yeast β-glucan conjugate showing the largest decrease in maximum fluorescence intensity, consistent with the results of DG. In addition, the significant redshift in the maximum emission wavelengths of the three conjugates indicates the movement of tryptophan residues to a hydrophilic environment during the coupling reaction (Sofronova et al., 2019).

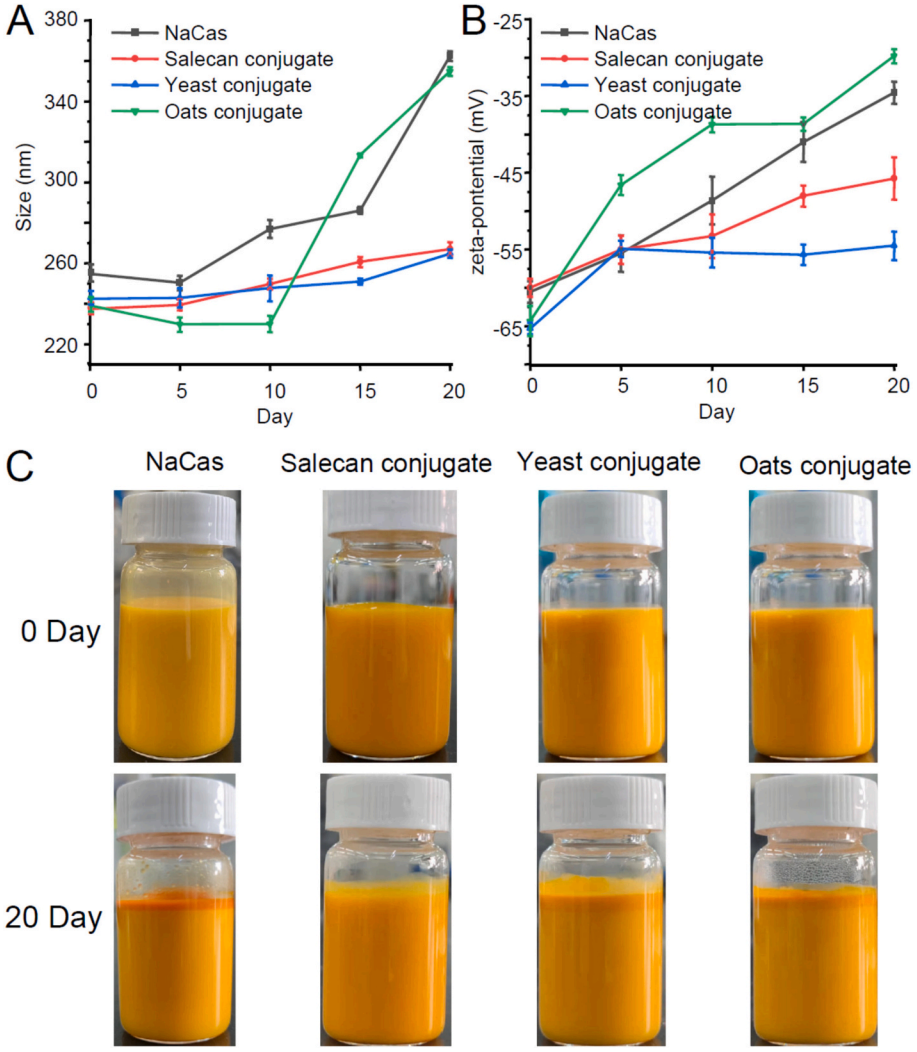

Fig. 4. Changes in the particle size (A) and ζ-potential (B) of sea buckthorn fruit oil nanoemulsions prepared with NaCas or three protein-polysaccharide conjugates at different storage times. (D) Visual images of sea buckthorn fruit oil nanoemulsions prepared with NaCas or three protein-polysaccharide conjugates after storage for 20 days. (NaCas: Nanoemulsion prepared with NaCas; Salecan conjugate: Nanoemulsion prepared with NaCas-Salecan conjugates; yeast conjugate: Nanoemulsion prepared with NaCas-yeast β-glucan conjugates; oat conjugate: Nanoemulsion prepared with NaCas-oat β-glucan conjugates).

Typically, such outcomes signify that the glycosylation reaction induces irreversible changes in the protein's secondary structure (Ding et al., 2023).

Furthermore, CD spectroscopy (Supplementary Fig. 1 A-D) revealed significant differences in the spectra of the three conjugates compared to NaCas, suggesting an alteration in the secondary structure of the protein due to β-glucan coupling. Analysis of protein secondary structures (Table 1) indicated mainly a decrease in β-sheet content and an increase in β-turns and random coils in the conjugates. Such modifications promote the formation of intermolecular hydrogen bonds and exposure of hydrophobic amino acid residues (Abd El-Salam & El-Shibiny, 2020). Flexibility and surface hydrophobicity are recognized as pivotal structural factors influencing the interfacial properties of emulsifiers. The Maillard reaction can disrupt various structural interactions in proteins, including hydrophobic interactions, hydrogen bonds, electrostatic attractions, van der Waals forces, and covalent bonds, rendering them more flexible (Nooshkam et al., 2023). Consequently, conjugates exhibiting higher surface hydrophobicity can enhance the hydrophobic interaction between oil droplets and proteins, facilitating a quicker reduction in interfacial tension. This phenomenon is advantageous for the formation and stability of emulsions (Nooshkam & Varidi, 2020).

3.2. Characteristics of sea buckthorn fruit oil nanoemulsions

The infrared spectra of the nanoemulsions depicted in Fig. 2 revealed characteristic peaks corresponding to NaCas and sea buckthorn fruit oil. NaCas exhibited characteristic peaks at 1635 cm^{-1} (C═O stretching) and 1515 cm^{-1} (C—N stretching) (Masoumi, Tabibiazar, Fazelioskouei, Mohammadifar, & Hamishehkar, 2023), while the 1100–1000 cm^{-1} region displayed typical peaks associated with the C-O-C stretching vibration of the sugar molecule in the glycosylated conjugate (Li, Li, Han, Zeng and Han, 2023). The characteristic peaks of sea buckthorn fruit oil included the C—H stretching vibration peaks of saturated carbon at 2925 and 2854 cm^{-1}, the C═O stretching vibration peak at 1746 cm^{-1}, the methylene bending vibration peak at 1464 cm^{-1}, the carbon chain skeleton vibration peak at 722 cm^{-1}, and the C—O stretching vibration peak in triglycerides at 1165 cm^{-1} (Mousa et al., 2022). All four nanoemulsions exhibited characteristic peaks of both NaCas and sea buckthorn fruit oil, indicating successful preparation.

Steric and electrostatic repulsion play crucial roles in stabilizing emulsions formed by protein-polysaccharide conjugates (Jiang et al., 2023). Larger particle sizes in oil-in-water (O/W) emulsions tend to diminish steric repulsion (Cheng, Xu, Wen, & Chen, 2005). Surface charge directly influences electrostatic repulsion. Table 2 presents the

Table 3
Changes in the fatty acid content of sea buckthorn fruit oil during storage.

	Storage time (day)	Palmitic acid ($C_{16:0}$) (%)	Palmitoleic acid ($C_{16:1}$) (%)	Stearic acid ($C_{18:0}$) (%)	Oleic acid ($C_{18:1}$) (%)	Linoleic acid ($C_{18:2}$) (%)	Linolenic acid ($C_{18:3}$) (%)	SFA (%)	MUFA (%)	PUFA (%)
Oil	0	30.95 ± 0.21^{d}	32.88 ± 0.24^{ab}	2.19 ± 0.01^{i}	10.94 ± 0.05^{d}	9.02 ± 0.02^{a}	14.02 ± 0.06^{a}	33.14 ± 0.22^{f}	43.82 ± 0.29^{a}	23.04 ± 0.08^{ab}
	20	34.95 ± 0.54^{a}	33.66 ± 0.46^{a}	2.79 ± 0.03^{d}	9.58 ± 0.02^{g}	6.74 ± 0.01^{f}	12.28 ± 0.12^{d}	37.74 ± 0.57^{a}	43.24 ± 0.48^{a}	19.02 ± 0.13^{e}
NaCas	0	30.72 ± 0.27^{d}	32.11 ± 0.32^{bc}	2.6 ± 0.05^{f}	11.37 ± 0.03^{ab}	8.84 ± 0.01^{b}	14.36 ± 0.04^{a}	33.32 ± 0.32^{ef}	43.48 ± 0.35^{a}	23.2 ± 0.05^{a}
	20	31.96 ± 0.61^{c}	32.08 ± 0.72^{bc}	3.62 ± 0.05^{a}	10.76 ± 0.04^{e}	8.15 ± 0.06^{d}	13.43 ± 0.13^{b}	35.58 ± 0.66^{c}	42.84 ± 0.76^{a}	21.58 ± 0.19^{c}
Salecan conjugate	0	31.04 ± 0.34^{d}	32.28 ± 0.27^{bc}	2.49 ± 0.00^{g}	11.21 ± 0.04^{bc}	8.87 ± 0.02^{ab}	14.12 ± 0.06^{a}	33.53 ± 0.34^{def}	43.49 ± 0.31^{a}	22.99 ± 0.08^{ab}
	20	30.98 ± 0.46^{d}	31.6 ± 0.71^{c}	3.45 ± 0.02^{b}	11.12 ± 0.14^{c}	8.84 ± 0.06^{b}	14.01 ± 0.13^{a}	34.43 ± 0.48^{d}	42.72 ± 0.85^{a}	22.85 ± 0.19^{ab}
Yeast conjugate	0	31.24 ± 0.45^{cd}	32.13 ± 0.52^{bc}	2.42 ± 0.01^{h}	11.3 ± 0.01^{ab}	8.9 ± 0.07^{ab}	14.19 ± 0.04^{a}	33.66 ± 0.46^{def}	43.43 ± 0.53^{a}	23.05 ± 0.11^{ab}
	20	30.73 ± 0.69^{d}	31.88 ± 0.61^{c}	3.37 ± 0.01^{c}	11.08 ± 0.14^{cd}	8.53 ± 0.07^{c}	14.04 ± 0.23^{a}	34.1 ± 0.7^{de}	42.96 ± 0.75^{a}	22.58 ± 0.32^{b}
Oats conjugate	0	30.52 ± 0.37^{d}	31.88 ± 0.34^{c}	2.64 ± 0.01^{e}	11.44 ± 0.12^{a}	8.94 ± 0.02^{ab}	14.17 ± 0.08^{a}	33.16 ± 0.38^{ef}	43.32 ± 0.46 ^{a}	23.11 ± 0.10^{a}
	20	33.47 ± 0.64^{b}	32.47 ± 0.58^{bc}	3.37 ± 0.02^{c}	10.41 ± 0.14^{f}	7.32 ± 0.05^{e}	12.96 ± 0.21^{c}	36.84 ± 0.66 ^{b}	42.88 ± 0.72 ^{a}	20.28 ± 0.26^{d}

Data presented are expressed as the mean ± SEM (n = 3). The different letters in each column represent a significant difference at $P < 0.05$. Oil: sea buckthorn fruit oil; NaCas: Nanoemulsion prepared with NaCas; Salecan conjugate: Nanoemulsion prepared with NaCas-Salecan conjugates; Yeast conjugate: Nanoemulsion prepared with NaCas-yeast β-glucan conjugates; Oats conjugate: Nanoemulsion prepared with NaCas-oat β-glucan conjugates.

particle size, PDI, and ζ-potential of the nanoemulsions. Nanoemulsions prepared with the conjugates exhibited superior characteristics compared to those prepared with the corresponding mixtures or NaCas in terms of particle size, PDI, and ζ-potential. This suggests that the enhanced emulsification properties of the conjugates stem from augmented steric and electrostatic repulsion. The observed variations among emulsions prepared with different conjugates also suggest the influence of the structure and source of β-glucan on the emulsifying properties of the prepared conjugates.

3.3. Nanoemulsion stability analysis

3.3.1. Effect of the pH on nanoemulsion stability

Electrostatic repulsion is the primary mechanism that prevents emulsion flocculation, but it is highly sensitive to pH changes. Near the protein's isoelectric point, emulsion flocculation occurs due to inadequate electrostatic repulsion (McClements & Gumus, 2016). The appearance, particle size and ζ-potential of the four nanoemulsions at different pH values are depicted in Supplementary Fig. 2 and Fig. 3A and B. When the pH crossed the isoelectric point of casein (pI = 4.6), all the nanoemulsions except for the those prepared with the NaCas-Salecan conjugates exhibited noticeable flocculation stratification. Concurrently, there was a significant increase in particle size, indicating inadequate electrostatic repulsion near the isoelectric point and insufficient steric hindrance to stabilize the emulsion (McClements & Gumus, 2016). When the pH decreased from 7.0 to 3.0, the surface net charge of these nanoemulsions also shifted from negative to positive, whereas the preparation of nanoemulsions with glycosylated conjugates delayed the pH-dependent change in ζ-potential. This delay was attributed to the covalent and noncovalent binding of proteins to polysaccharides, which decreased the isoelectric point of casein (Wooster & Augustin, 2007). Remarkably, the nanoemulsions prepared with NaCas-Salecan conjugates did not exhibit obvious flocculation stratification at any pH, and the changes in particle size and ζ-potential were minimal. This indicated that NaCas-Salecan conjugates were more effective in inhibiting attractive interactions and aggregation between droplets during emulsion preparation. This phenomenon may be attributed to the positively correlated between the thickness of the interface formed by the conjugates and the molecular weight of the polysaccharide. Larger-molecular-weight polysaccharides provided greater steric repulsion during the formation of glycosylated conjugates, thereby preventing coalescence and aggregation of emulsions (Fan, Yi, Zhang, Wen, & Zhao, 2017; McClements & Gumus, 2016).

3.3.2. Effect of temperature on the nanoemulsion stability

The changes in nanoemulsion particle size and ζ-potential at different temperatures are shown in Fig. 3C and D. The particle sizes of the nanoemulsions prepared with NaCas-Salecan conjugates and NaCas-yeast β-glucan conjugates exceeded those of NaCas, possibly due to increased electrostatic repulsion and steric hindrance induced by glycosylation, which augmented negative charges around the protein (Sriprablom, Luangpituksa, Wongkongkatep, Pongtharangkul, & Suphantharika, 2019). However, the ζ-potentials of these nanoemulsions remained above −30 mV at all temperatures, indicating their relative stability and ability to withstand pasteurization from 30 to 90 °C.

3.3.3. Effect of bile salts on nanoemulsion stability

Bile salts play a crucial role in promoting the digestion and absorption of fat-soluble nutrients (Liu et al., 2019). The effect of bile salts on nanoemulsions is shown in Fig. 3E and F. With increasing bile salt concentration, the particle size initially increased and then decreased. This phenomenon is attributed to bile salts shielding some surface charges on the emulsion, thus weakening electrostatic repulsion between droplets (Romanski, 2007). However, due to the synergistic effect of bile salts as emulsifiers with NaCas, the nanoemulsion particle size decreased at higher bile salt concentrations (Dickinson, 2010). The ζ-potential of the nanoemulsions gradually decreased with increasing

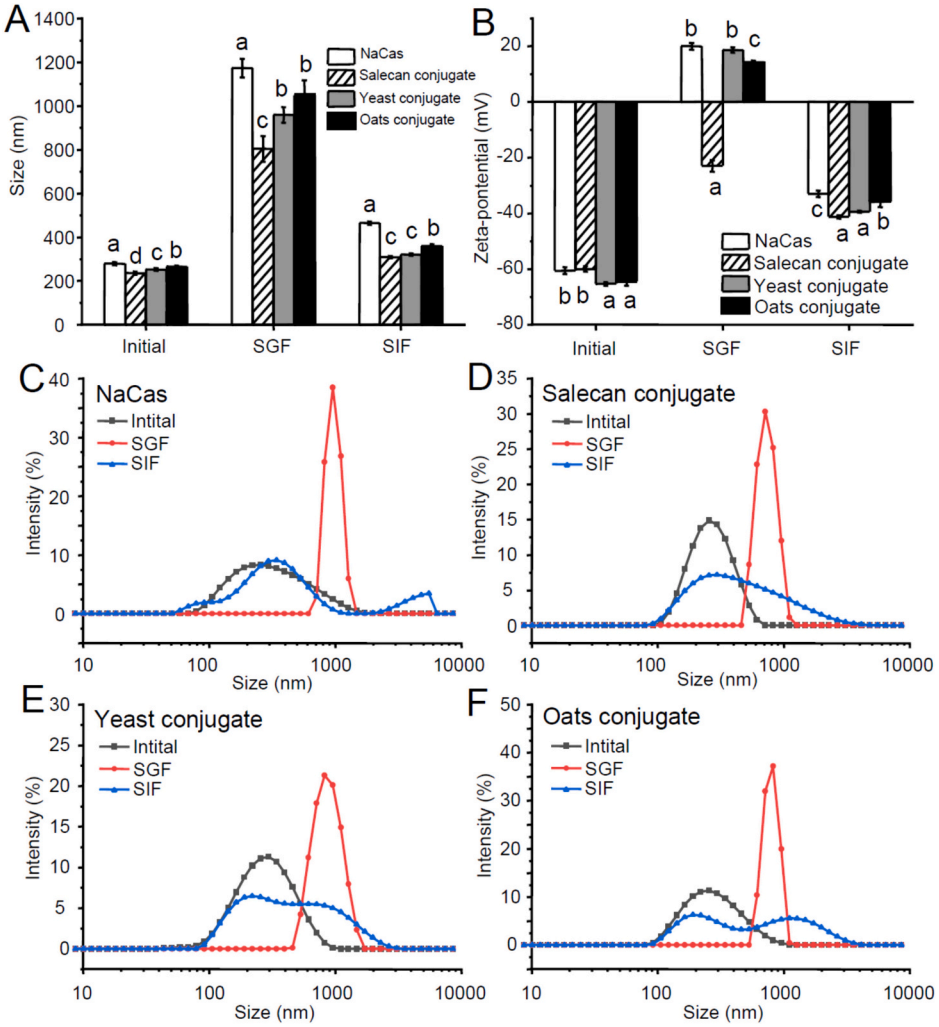

Fig. 5. Changes in the particle size (A) and ζ-potential (B) of sea buckthorn fruit oil nanoemulsions prepared with NaCas or three protein-polysaccharide conjugates during *in vitro* digestion. (C ~ F) Changes in the particle size distribution of nanoemulsions prepared with NaCas or three protein-polysaccharide conjugates during *in vitro* digestion. Data presented are expressed as the mean ± SEM (n = 3). The different letters in same digestive stage represent a significant difference at $P < 0.05$. (NaCas: Nanoemulsion prepared with NaCas; Salecan conjugate: Nanoemulsion prepared with NaCas-Salecan conjugates; yeast conjugate: Nanoemulsion prepared with NaCas-yeast β-glucan conjugates; oat conjugate: Nanoemulsion prepared with NaCas-oat β-glucan conjugates).

bile salt concentration, which was consistent with previous studies and may be due to the electrostatic shielding effect caused by bile salts (Sarkar, Ye, & Singh, 2016). Notably, the stability of the nanoemulsions prepared with NaCas-Salecan conjugates and NaCas-oat conjugates exhibited significantly better stability than those of the nanoemulsions prepared with NaCas, indicating that the polysaccharide conjugates effectively enhance emulsion stability by increasing the steric and electrostatic repulsion.

3.3.4. Storage stability of nanoemulsions

The appearance, particle size and ζ-potential of the nanoemulsions stored at room temperature for 20 days after pasteurization are shown in Fig. 4. With increased storage time, all nanoemulsions experienced gradual particle size increases and ζ-potential absolute value decreases. Notably, nanoemulsions prepared with NaCas-Salecan and NaCas-yeast β-glucan conjugates exhibited less pronounced changes during this period. However, by the 20th day, except for the nanoemulsion prepared with NaCas-Salecan conjugates, all other nanoemulsions appeared a visual phase separation.

Nanoemulsions are thermodynamically unstable colloidal dispersions (Fan et al., 2017). Over time, alterations in protein conformation at the interfacial layer and interactions with the two phases promote droplet flocculation by increasing hydrophobic attraction and forming disulfide bonds between proteins located in different droplets (Ozturk & McClements, 2016). Protein-polysaccharide conjugates, with optimized hydrophilic-lipophilic balance, envelop oil droplets, inhibiting aggregation and flocculation during storage *via* electrostatic and steric repulsion(Seidi, Nasirpour, Keramat, & Saeidy, 2023). Additionally, the viscosity increase of proteins post-glycosylation reduces the gravitational separation rate and Brownian motion of oil droplets, contributing to emulsion stability(Nooshkam et al., 2023). Polysaccharides with higher molecular weights yield conjugates with elevated viscosities (Dunlap, Côté, & Chemistry, 2005). The higher molecular weight of Salecan compared to other β-glucans may be the reason for the better storage stability of nanoemulsions prepared with NaCas-Salecan conjugates.

3.4. Changes in of fatty acid composition during storage

Sea buckthorn fruit oil, rich in unsaturated fatty acids (UFAs), suffers from poor stability (Caballero & Davidov-Pardo, 2021). The changes in the fatty acid composition of sea buckthorn fruit oil after 20 days of storage at room temperature are shown in Table 3. Nanoemulsion preparation did not alter the fatty acid composition of the oil. However,

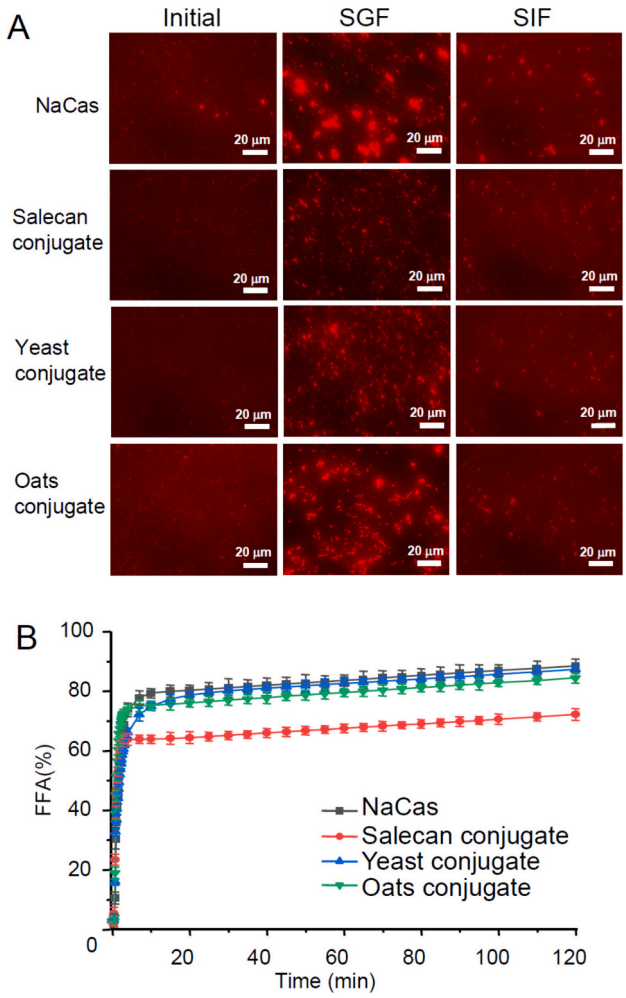

Fig. 6. (A) Micromorphological changes in the nanoemulsions during *in vitro* digestion. (B) The free fatty acid release rate of the nanoemulsions during the intestinal digestion stage.

storage led to increased saturated fatty acids (SFAs) and decreased polyunsaturated fatty acids (PUFAs) in sea buckthorn fruit oil, indicative of oxidation converting PUFAs into monounsaturated fatty acids (MUFAs) or SFAs during storage (Waglewska et al., 2022). In contrast, the fatty acid content in the four nanoemulsions changed less, suggesting effective PUFA preservation. Notably, the relative content of unsaturated fatty acids in the nanoemulsions prepared with NaCas-Salecan conjugates and NaCas-yeast conjugates did not change significantly after storage. Some studies have shown significant differences in the antioxidant activity (oxygen radical absorbance capacity and ferric reducing antioxidant power) of β-glucans with various MWs and from different sources, although the antioxidant mechanism of β-glucan was not clear (Minekus et al., 2014). These findings suggest that nanoemulsions formulated with NaCas-Salecan and NaCas-yeast conjugates may offer enhanced antioxidant efficacy, thus effectively preserving the functional components of sea buckthorn fruit oil.

3.5. Characteristics of the nanoemulsion in vitro digestion model

The nanoemulsions underwent various degrees of damage during *in vitro* digestion, leading to phenomena such as flocculation, aggregation, and demulsification, as depicted in Fig. 5 and 6A. In the gastric digestion stage, significant increases in particle size and droplet aggregation occurred due to reduced electrostatic repulsion in the low-pH environment of simulated gastric fluid (Lv, Shi, Binks, Jiang, & Cui, 2023). In particular, the nanoemulsions prepared with NaCas exhibited the largest changes in particle size and aggregation, likely due to NaCas hydrolysis by pepsin, exposing oil droplets and promoting aggregation (Liu et al., 2019). Conversely, glycosylation products exhibited high electrostatic repulsion and steric hindrance, inhibiting pepsin hydrolysis to some extent (Kenmogne-Domguia, Meynier, Viau, Llamas, & Genot, 2012). Interestingly, except for the nanoemulsions prepared with NaCas-Salecan conjugates, the other nanoemulsions were positively charged, possibly due to the electrostatic shielding effect of SGF's greater ionic strength (Davidov-Pardo, Perez-Ciordia, Marin-Arroyo, & McClements, 2015). The nanoemulsions prepared with NaCas-Salecan conjugates can maintained a negative potential and had the lowest degree of aggregation in SGF, attributed to Salecan's higher molecular weight and strong steric hindrance.

During the intestinal digestion stage, all nanoemulsions exhibited decreased particle sizes, reduced aggregation, and diminished fluorescence brightness compared to the gastric digestion stage, likely due to bile salts replacing the interfacial layer and promoting the lipase to enter the interior of the oil droplets. Bile salts could also adsorb to form a new emulsion interface, reducing particle size (Lin, Liang, Williams, & Zhong, 2018). At the same time, the significantly chang in ζ-potential may result from the neutral environment of SIF and the adsorption of anionic colloidal particles (bile salts, free fatty acids and peptides) (Zhang, Zhang, Zhang, Decker, & McClements, 2015). As shown in Fig. 5 (C—F), the particle size distributions became broader with bimodal or multimodal distributions, indicating the presence of various colloidal particles, such as undigested oil droplets, micelles, and undissolved calcium salts (Lin et al., 2018).

To understand the release of sea buckthorn fruit oil in the nanoemulsions during the intestinal digestion stage, the free fatty acid release rate was detected using the pH-stat method, and the results are shown in Fig. 6B. The oil in all the nanoemulsions was rapidly digested by lipase within 10 min, with the release rate stabilizing thereafter. Nanoemulsions prepared with the NaCas-Salecan conjugates exhibited significantly lower free fatty acid release rates, likely due to higher viscosity and thicker interfacial layers inhibiting lipase entry and fat hydrolysis (McClements, Decker, & Park, 2009). Similar studies have shown that the release rate of fatty acids was inversely proportional to the molecular weight of glycosylated polysaccharides (Lesmes & McClements, 2012). In addition, increased release of fatty acids during gastric and intestinal digestion stages leads to decreased fat delivery to the colorectum (Li, Hwang, Chen, & Park, 2016). Droplet interfacial composition and properties play a crucial role in altering the *in vitro* digestion process of emulsions with similar mean particle sizes and PDIs (McClements et al., 2009). These results highlight the superior stability of nanoemulsions prepared with the glycosylation products compared to those with NaCas during *in vitro* digestion. Particularly, nanoemulsions prepared with the NaCas-Salecan conjugates exhibited minimal aggregation, high digestion resistance, and superior stability, suggesting potential for targeted delivery of sea buckthorn fruit oil to the colorectum.

4. Conclusion

In this study, β-glucan from three different sources were utilized to prepare protein-polysaccharide conjugates with NaCas, serving as interface materials for sea buckthorn fruit oil nanoemulsions. These conjugates were formed through covalent coupling reactions, altering the secondary structure of casein. Nanoemulsions prepared with glycosylation conjugates exhibited superior stability compared to those with NaCas. Among them, the nanoemulsions prepared with NaCas-Salecan conjugates demonstrating the highest stability and antioxidant effects on unsaturated fatty acids in sea buckthorn fruit oil. This enhanced stability and antioxidant activity can be attributed to the electrostatic repulsion and steric hindrance generated by the high molecular weight of Salecan. *In vitro* digestion experiments also corroborated the superior stability of nanoemulsions prepared with the NaCas-Salecan conjugates,

exhibiting minimal emulsion aggregation, flocculation, and a lower release rate of fatty acids. Consequently, sea buckthorn fruit oil nanoemulsions formulated with NaCas-Salecan conjugates offer prolonged storage stability, enhanced emulsion stability, and the potential for colorectal-targeted delivery in functional foods. However, their *in vivo* bioavailability and impact on gut microbiota need to be explored in further studies.

CRediT authorship contribution statement

Ziyi Shen: Writing – original draft, Software, Data curation, Conceptualization. **Xinyue Yang:** Methodology, Conceptualization. **Yao Liu:** Writing – original draft, Methodology. **Lei Liu:** Methodology, Data curation. **YuKun Huang:** Software, Methodology. **Pengfei Chen:** Writing – review & editing, Software. **Xianggui Chen:** Supervision, Software, Funding acquisition. **Chisong Zhang:** Software, Resources. **Juan Zhao:** Writing – review & editing, Software, Investigation, Data curation. **Xiao Yang:** Writing – review & editing, Project administration, Funding acquisition. **Qin Wang:** Writing – review & editing, Software, Funding acquisition.

Declaration of competing interest

The authors have declared no conflict of interest or personal relationships that could have appeared to influence the work reported in this paper.

Data availability

No data was used for the research described in the article.

Acknowledgments

This work was supported by the National Natural Science Foundation of China [grant numbers 3197160117, 2020], the Sichuan Province Science and Technology Support Program [grant numbers 2022JDTD0028, 2022YFN0016].

Appendix A. Supplementary data

Supplementary data to this article can be found online at https://doi.org/10.1016/j.foodchem.2024.140098.

References

Abd El-Salam, M. H., & El-Shibiny, S. (2020). Preparation and potential applications of casein–polysaccharide conjugates: A review. *Journal of the Science of Food and Agriculture, 100*(5), 1852–1859. https://doi.org/10.1002/jsfa.10187

Borreani, J., Espert, M., Salvador, A., Sanz, T., Quiles, A., & Hernando, I. (2017). Oil-in-water emulsions stabilised by cellulose ethers: Stability, structure and in vitro digestion. *Food & Function, 8*(4), 1547–1557. https://doi.org/10.1039/C7FO00159B

Caballero, S., & Davidov-Pardo, G. (2021). Comparison of legume and dairy proteins for the impact of Maillard conjugation on nanoemulsion formation, stability, and lutein color retention. *Food Chemistry, 338*(9), Article 128083. https://doi.org/10.1016/j.foodchem.2020.128083

Capar, T. D., & Yalcin, H. (2021). Protein/polysaccharide conjugation via Maillard reactions in an aqueous media: Impact of protein type, reaction time and temperature. *Lwt-Food Science and Technology, 152*(8), Article 112252. https://doi.org/10.1016/j.lwt.2021.112252

Chang, M., Guo, Y., Jiang, Z., Shi, L., Zhang, T., Wang, Y., Gong, M., Wang, T., Lin, R., Liu, R., Wang, Y., Jin, Q., & Wang, X. (2020). Sea buckthorn pulp oil nanoemulsions fabricated by ultra-high pressure homogenization process: A promising carrier for nutraceutical. *Journal of Food Engineering, 287*(5), Article 110129. https://doi.org/10.1016/j.jfoodeng.2020.110129

Cheng, J., Xu, S., Wen, L., & Chen, J. J. L. (2005). *Steric repulsion between internal aqueous droplets and the external aqueous phase in double emulsions, 21*(25), 12047–12052. https://doi.org/10.1021/la051906r

Davidov-Pardo, G., Perez-Ciordia, S., Marin-Arroyo, M. R., & McClements, D. J. (2015). Improving resveratrol bioaccessibility using biopolymer nanoparticles and complexes: Impact of protein-carbohydrate maillard conjugation. *Journal of Agricultural and Food Chemistry, 63*(15), 3915–3923. https://doi.org/10.1021/acs.jafc.5b00777

Dickinson, E. (2010). Flocculation of protein-stabilized oil-in-water emulsions. *Colloids and Surfaces B-Biointerfaces, 81*(1), 130–140. https://doi.org/10.1016/j.colsurfb.2010.06.033

Ding, H., Yan, H., Yu, Z., & Liu, L. (2023). Spectroscopic analysis of the effect of glycation on casein structure and aggregation and its dependence on lactose concentration. *Food Chemistry, 404*, Article 134679. https://doi.org/10.1016/j.foodchem.2022.134679

Dong, K., Binosha Fernando, W. M. A. D., Durham, R., Stockmann, R., & Jayasena, V. (2023). Nutritional value, health-promoting benefits and food application of sea buckthorn. *Food Reviews International, 39*(4), 2122–2137. https://doi.org/10.1080/87559129.2021.1943429

Dunlap, C. A., Côté, G. L. J. J. O. A., & Chemistry, F. (2005). *β-Lactoglobulin– dextran conjugates: effect of polysaccharide size on emulsion stability. 53(2), 419–423*. https://doi.org/10.1021/jf049180c

Fan, Y., Yi, J., Zhang, Y., Wen, Z., & Zhao, L. (2017). Physicochemical stability and invitro bioaccessibility of β-carotene nanoemulsions stabilized with whey protein-dextran conjugates. *Food Hydrocolloids, 63*(2), 256–264. https://doi.org/10.1016/j.foodhyd.2016.09.008

Islam, F., Saeed, F., Afzaal, M., Hussain, M., Ikram, A., & Khalid, M. A. (2023). Food grade nanoemulsions: Promising delivery systems for functional ingredients. *Journal of Food Science and Technology, 60*(5), 1461–1471. https://doi.org/10.1007/s13197-022-05387-3

Jiang, Z., Huangfu, Y., Jiang, L., Wang, T., Bao, Y., & Ma, W. (2023). Structure and functional properties of whey protein conjugated with carboxymethyl cellulose through maillard reaction. *LWT, 174*, Article 114406. https://doi.org/10.1016/j.lwt.2022.114406

Kaur, R., Sharma, M., Ji, D., Xu, M., & Agyei, D. (2020). Structural features, modification, and functionalities of beta-glucan. *Fibers, 8*(1), 1. https://doi.org/10.3390/fib8010001

Kenmogne-Domguia, H. B., Meynier, A., Viau, M., Llamas, G., & Genot, C. (2012). Gastric conditions control both the evolution of the organization of protein-stabilized emulsions and the kinetic of lipolysis during in vitro digestion. *Food & Function, 3*(12), 1302–1309. https://doi.org/10.1039/c2fo30031a

Lesmes, U., & McClements, D. J. (2012). Controlling lipid digestibility: Response of lipid droplets coated by β-lactoglobulin-dextran Maillard conjugates to simulated gastrointestinal conditions. *Food Hydrocolloids, 26*(1), 221–230. https://doi.org/10.1016/j.foodhyd.2011.05.011

Li, J., Hwang, I.-C., Chen, X., & Park, H. J. (2016). Effects of chitosan coating on curcumin loaded nano-emulsion: Study on stability and in vitro digestibility. *Food Hydrocolloids, 60*(10), 138–147. https://doi.org/10.1016/j.foodhyd.2016.03.016

Li, Y., Li, D.-M., Han, Y., Zeng, X.-A., & Han, Z. (2023). Structural and functional properties of sodium caseinate glycosylated by dextran aldehyde. *Food Chemistry, 404*(10), Article 134589. https://doi.org/10.1016/j.foodchem.2022.134589

Lin, Q., Liang, R., Williams, P. A., & Zhong, F. (2018). Factors affecting the bioaccessibility of β-carotene in lipid-based microcapsules: Digestive conditions, the composition, structure and physical state of microcapsules. *Food Hydrocolloids, 77*(4), 187–203. https://doi.org/10.1016/j.foodhyd.2017.09.034

Liu, J., Liu, W., Salt, L. J., Ridout, M. J., Ding, Y., & Wilde, P. J. (2019). Fish oil emulsions stabilized with caseinate glycated by dextran: Physicochemical stability and gastrointestinal fate. *Journal of Agricultural and Food Chemistry, 67*(1), 452–462. https://doi.org/10.1021/acs.jafc.8b04190

Liu, W., Gao, H., Mcclements, D. J., Zhou, L., Wu, J., & Zou, L. (2019). Stability, rheology, and β-carotene bioaccessibility of high internal phase emulsion gels. *Food Hydrocolloids, 88*(3), 210–217. https://doi.org/10.1016/j.foodhyd.2018.10.012

Lv, M., Shi, J., Binks, B. P., Jiang, J., & Cui, Z. (2023). Competition between hydrogen bonding and electrostatic repulsion in pH-switchable emulsions. *Journal of Molecular Liquids, 390*(9), Article 123095. https://doi.org/10.1016/j.molliq.2023.123095

Masoumi, B., Tabibiazar, M., Fazelioskouei, T., Mohammadifar, M., & Hamishehkar, H. (2023). Pickering emulsion stabilized by conjugated sodium caseinate-ascorbic acid nanoparticles: Synthesis and physicochemical characterization. *Food Hydrocolloids, 145*(8), Article 109168. https://doi.org/10.1016/j.foodhyd.2023.109168

McClements, D. J., Decker, E. A., & Park, Y. (2009). Controlling lipid bioavailability through physicochemical and structural approaches. *Critical Reviews in Food Science and Nutrition, 49*(1), 48–67. https://doi.org/10.1080/10408390701764245

McClements, D. J., & Gumus, C. E. (2016). Natural emulsifiers - biosurfactants, phospholipids, biopolymers, and colloidal particles: Molecular and physicochemical basis of functional performance. *Advances in Colloid and Interface Science, 234*(8), 3–26. https://doi.org/10.1016/j.cis.2016.03.002

Minekus, M., Alminger, M., Alvito, P., Ballance, S., Bohn, T., Bourlieu, C., Carrière, F., Boutrou, R., Corredig, M., & Dupont, D. (2014). A standardised static in vitro digestion method suitable for food–an international consensus. *Food & Function, 5*(6), 1113–1124. https://doi.org/10.1039/C3FO60702J

Mirdha, L., & Chakraborty, H. (2019). Characterization of structural conformers of κ-casein utilizing fluorescence spectroscopy. *International Journal of Biological Macromolecules, 131*, 89–96. https://doi.org/10.1016/j.ijbiomac.2019.03.040

Mousa, M. A. A., Wang, Y., Antora, S. A., Al-Qurashi, A. D., Ibrahim, O. H. M., He, H. J., … Kamruzzaman, M. (2022). An overview of recent advances and applications of FT-IR spectroscopy for quality, authenticity, and adulteration detection in edible oils. *Critical Reviews in Food Science and Nutrition, 62*(29), 8009–8027. https://doi.org/10.1080/10408398.2021.1922872

Nooshkam, M., & Varidi, M. (2020). Whey protein isolate-low acyl gellan gum Maillard-based conjugates with tailored technological functionality and antioxidant activity. *International Dairy Journal, 109*, Article 104783. https://doi.org/10.1016/j.idairyj.2020.104783

Nooshkam, M., Varidi, M., Zareie, Z., & Alkobeisi, F. (2023). Behavior of protein-polysaccharide conjugate-stabilized food emulsions under various destabilization

conditions. *Food Chemistry: X, 18*, Article 100725. https://doi.org/10.1016/j.fochx.2023.100725

Olas, B. (2018). The beneficial health aspects of sea buckthorn (Elaeagnus rhamnoides (L.) a.Nelson) oil. *Journal of Ethnopharmacology, 213*(3), 183–190. https://doi.org/10.1016/j.jep.2017.11.022

de Oliveira, F. C., Coimbra, J. S. D., de Oliveira, E. B., Zuniga, A. D. G., & Rojas, E. E. G. (2016). Food protein-polysaccharide conjugates obtained via the maillard reaction: A review. *Critical Reviews in Food Science and Nutrition, 56*(7), 1108–1125. https://doi.org/10.1080/10408398.2012.755669

Ozturk, B., & McClements, D. J. (2016). Progress in natural emulsifiers for utilization in food emulsions. *Current Opinion in Food Science, 7*, 1–6. https://doi.org/10.1016/j.cofs.2015.07.008

Rave, M. C., Echeverri, J. D., & Salamanca, C. H. (2020). Improvement of the physical stability of oil-in-water nanoemulsions elaborated with Sacha inchi oil employing ultra-high-pressure homogenization. *Journal of Food Engineering, 273*(5), Article 109801. https://doi.org/10.1016/j.jfoodeng.2019.109801

Romanski, K. W. (2007). The role and mechanism of action of bile acids within the digestive system - bile acids in the liver and bile. *Advances in Clinical and Experimental Medicine, 16*(6), 793–799.

Sarkar, A., Ye, A., & Singh, H. (2016). On the role of bile salts in the digestion of emulsified lipids. *Food Hydrocolloids, 60*(10), 77–84. https://doi.org/10.1016/j.foodhyd.2016.03.018

Seidi, P., Nasirpour, A., Keramat, J., & Saeidy, S. (2023). Functional and structural properties of gum arabic complexes with casein and hydrolyzed casein achieved by Maillard reaction. *Journal of Dispersion Science and Technology, 44*(4), 639–650. https://doi.org/10.1080/01932691.2021.1958686

Sofronova, A., Semenyuk, P., & Muronetz, V. (2019). The influence of β-casein glycation on its interaction with natural and synthetic polyelectrolytes. *Food Hydrocolloids, 89*, 425–433. https://doi.org/10.1016/j.foodhyd.2018.11.011

Sriprablom, J., Luangpituksa, P., Wongkongkatep, J., Pongtharangkul, T., & Suphantharika, M. (2019). Influence of pH and ionic strength on the physical and rheological properties and stability of whey protein stabilized o/w emulsions containing xanthan gum. *Journal of Food Engineering, 242*(2), 141–152. https://doi.org/10.1016/j.jfoodeng.2018.08.031

Sun, T., Qin, Y., Xie, J., Xu, H., Gan, J., Wu, J., Bian, X., Li, X., Xiong, Z., & Xue, B. (2019). Effect of Maillard reaction on rheological, physicochemical and functional properties of oat β-glucan. *Food Hydrocolloids, 89*(4), 90–94. https://doi.org/10.1016/j.foodhyd.2018.10.029

Tereshchuk, L. V., Starovoitova, K. V., Vyushinsky, P. A., & Zagorodnikov, K. A. (2022). The use of sea buckthorn processing products in the creation of a functional biologically active food emulsion. *Foods, 11*(15), 2226. https://doi.org/10.3390/foods11152226

Vilas-Franquesa, A., Saldo, J., & Juan, B. (2020). Potential of sea buckthorn-based ingredients for the food and feed industry - a review. *Food Production Processing and Nutrition, 2*(1), 1–17. https://doi.org/10.1186/s43014-020-00032-y

Waglewska, E., Misiaszek, T., & Bazylinska, U. (2022). Nanoencapsulation of poorly soluble sea-buckthorn pulp oil in bile salt-origin vesicles: Physicochemical characterization and colloidal stability. *Colloids and Surfaces a-Physicochemical and Engineering Aspects, 647*(4), Article 129113. https://doi.org/10.1016/j.colsurfa.2022.129113

Wang, K., Xu, Z., & Liao, X. (2022). Bioactive compounds, health benefits and functional food products of sea buckthorn: A review. *Critical Reviews in Food Science and Nutrition, 62*(24), 6761–6782. https://doi.org/10.1080/10408398.2021.1905605

Wooster, T. J., & Augustin, M. A. (2007). The emulsion flocculation stability of protein-carbohydrate diblock copolymers. *Journal of Colloid and Interface Science, 313*(2), 665–675. https://doi.org/10.1016/j.jcis.2007.04.054

Xu, J., Mukherjee, D., & Chang, S. K. C. (2018). Physicochemical properties and storage stability of soybean protein nanoemulsions prepared by ultra-high pressure homogenization. *Food Chemistry, 240*(2), 1005–1013. https://doi.org/10.1016/j.foodchem.2017.07.077

Zhang, R., Zhang, Z., Zhang, H., Decker, E. A., & McClements, D. J. (2015). Influence of lipid type on gastrointestinal fate of oil-in-water emulsions: In vitro digestion study. *Food Research International, 75*(9), 71–78. https://doi.org/10.1016/j.foodres.2015.05.014

Zhang, S., Gong, Y., Khanal, S., Lu, Y., & Lucey, J. A. (2017). Properties of acid gels made from sodium caseinate-maltodextrin conjugates prepared by a wet heating method. *Journal of Dairy Science, 100*(11), 8744–8753. https://doi.org/10.3168/jds.2017-12602

Zheng, J., Sun, D., Li, X., Liu, D., Li, C., Zheng, Y., Yue, X., & Shao, J.-H. (2021). The effect of fatty acid chain length and saturation on the emulsification properties of pork myofibrillar proteins. *LWT, 139*, Article 110242. https://doi.org/10.1016/j.lwt.2020.110242